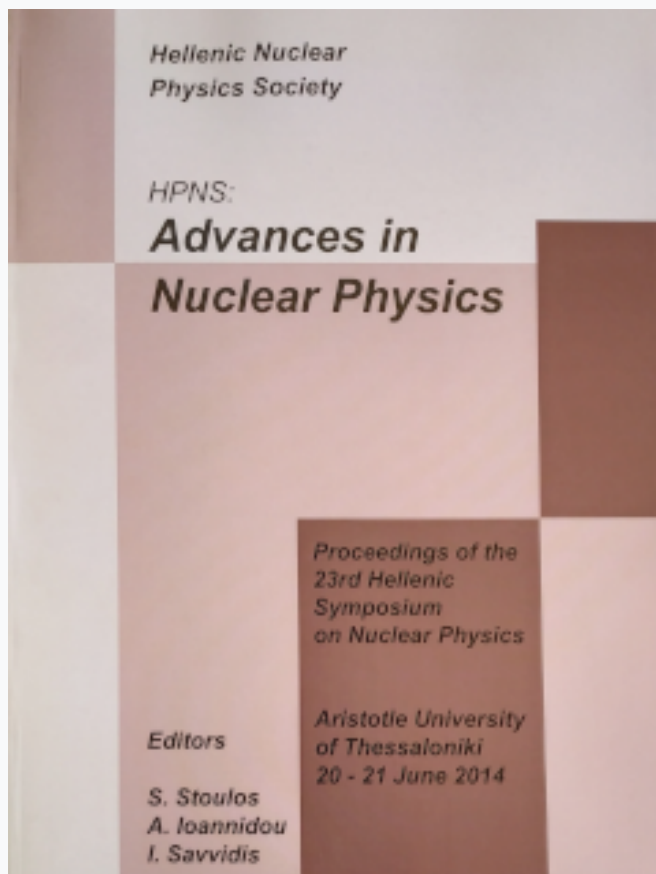


Annual Symposium of the Hellenic Nuclear Physics Society

Τόμ. 22 (2014)

HNPS2014



Measurement of the $^{237}\text{Np}(n,f)$ cross section with the FIC detector at the CERN n_TOF facility

M. Diakaki, et al. for the nTOF Collaboration

doi: [10.12681/hnps.1925](https://doi.org/10.12681/hnps.1925)

Βιβλιογραφική αναφορά:

Diakaki, M., & for the nTOF Collaboration, et al. (2019). Measurement of the $^{237}\text{Np}(n,f)$ cross section with the FIC detector at the CERN n_TOF facility. *Annual Symposium of the Hellenic Nuclear Physics Society*, 22, 20–27. <https://doi.org/10.12681/hnps.1925>

Measurement of the $^{237}\text{Np}(n,f)$ cross section with the FIC detector at the CERN n_TOF facility

M. Diakaki¹, D. Karadimos¹, R. Vlastou¹, M. Kokkoris¹, L. Audouin, U. Abbondanno, G. Aerts, H. Alvarez, F. Alvarez-Velarde, S. Andriamonje, J. Andrzejewski, P. Assimakopoulos[†], G. Badurek, P. Baumann, F. Becvar, F. Belloni, E. Berthoumieux, F. Calvino, M. Calviani, D. Cano-Ott, R. Capote, C. Carrapi, P. Cennini, V. Chepel, E. Chiaveri, N. Colonna, G. Cortes, A. Couture, J. Cox, M. Dahlfors, S. David, I. Dillmann, C. Domingo-Pardo, W. Dridi, I. Duran, C. Eleftheriadis, L. Ferrant[†], A. Ferrari, R. Ferreira-Marques, K. Fujii, W. Furman, S. Galanopoulos, I. F. Goncalves, E. Gonzalez-Romero, F. Gramegna, C. Guerrero, F. Gunsing, B. Haas, R. Haight, M. Heil, A. Herrera-Martinez, M. Igashira, E. Jericha, F. Kappeler, Y. Kadi, D. Karamanis, M. Kerveno, P. Koehler, V. Konovalov, E. Kossionides, M. Krlicka, C. Lampoudis, C. Lederer, H. Leeb, A. Lindote, I. Lopes, M. Lozano, S. Lukic, J. Marganec, S. Marrone, T. Martinez, C. Massimi, P. Mastinu, E. Mendoza, A. Mengoni, P.M. Milazzo, C. Moreau, M. Mosconi, F. Neves, H. Oberhummer, S. O'Brien, J. Pancin, C. Papadopoulos, C. Paradela, A. Pavlik, P. Pavlopoulos, G. Perdikakis, L. Perrot, M. T. Pigni, R. Plag, A. Plompen, A. Plukis, A. Poch, J. Praena, C. Pretel, J. Quesada, T. Rauscher, R. Reifarth, M. Rosetti, C. Rubbia, G. Rudolf, P. Rullhusen, L. Sarchiapone, R. Sarmiento, I. Savvidis, C. Stephan, G. Tagliente, J. L. Tain, L. Tassan-Got, L. Tavora, R. Terlizzi, G. Vannini, P. Vaz, A. Ventura, D. Villamarin, V. Vlachoudis, F. Voss, S. Walter, M. Wiescher and K. Wisshak

¹National Technical University of Athens, Athens, Greece
(The n_TOF collaboration www.cern.ch/ntof)

Abstract

The cross section of the $^{237}\text{Np}(n,f)$ reaction has been experimentally determined at the n_TOF facility at CERN, in the neutron energy range 100 keV – 10 MeV, relative to the standard $^{235}\text{U}(n,f)$ and $^{238}\text{U}(n,f)$ reaction cross sections with use of a Fast Ionisation Chamber. The reproduction of the high accuracy data obtained from this experiment was attempted within the Hauser-Feshbach formalism and phenomenological models with use of the code EMPIRE 3.2.

1. Introduction

There is an increasing need for accurate cross section data on neutron-induced reactions - especially fission- for nuclear technology applications, concerning the design of new systems for safe and clean energy production and nuclear waste transmutation, such as the subcritical Accelerator Driven Systems (ADS) or the future Generation-IV fast nuclear reactors. The long-lived ^{237}Np is the major component of the spent nuclear fuel in existing reactors, mainly produced by neutron captures in ^{235}U and $(n,2n)$ reactions in ^{238}U , thus the transmutation of this isotope is a very important issue. There is a number of data in literature on the $^{237}\text{Np}(n,f)$ reaction that present discrepancies up to 8% while the new evaluations ENDF/B-VII.1 [1], JEFF-3.2 [2], JENDL-4.0 [3] present differences up to 3% above 2 MeV.

The $^{237}\text{Np}(n,f)$ cross section has been measured, relative to ^{235}U and ^{238}U fission cross sections, at the n_TOF facility [4], CERN, from ~100 keV to 10 MeV. The most important features of this setup are the high instantaneous neutron flux and the excellent energy resolution. The fission fragments were detected with use of a fast ionization chamber (FIC) [5], and fast electronics were used, including Time to Digital Converters (TDC) and Flash Analog to Digital Converters (FADC). An adapted analysis procedure has been used [6] in order to obtain the reaction rate from each actinide. A phenomenological analysis of the cross section data has been attempted with the code

EMPIRE 3.2 [7,8] in an effort to simultaneously reproduce all the competing reaction channels.

2. Experimental procedure

The n_TOF facility (neutron Time-Of-Flight) [4] is located at CERN (European Organization for Nuclear Research) in Switzerland and has been designed and built from an international collaboration after a proposal from C. Rubbia et al. [9] in order to provide high accuracy neutron induced reaction cross section data for nuclear technology and nuclear astrophysics purposes. The white neutron beam at the CERN n_TOF facility is produced via the spallation process occurring from the collision of protons with a momentum of 20 GeV/c on a thick lead target. The high energy and high flux pulsed proton beam is provided by the Proton Synchrotron (PS) accelerator complex. Up to 7e12 ppp (protons per pulse) can be provided, in the form of short (7 ns width) pulses with a time interval of >4 s. The produced neutron beam from the spallation process is propagated in the TOF vacuum tube for approximately 185 m before entering the experimental area. In order to minimize the contamination of the neutron beam with primary protons, and other secondary particles, the proton beam line forms an angle of 10° relative to the TOF tube.

The features of the n_TOF facility at CERN that make it a unique neutron source facility worldwide is the high instantaneous flux maximizing the signal-to-background ratio, the excellent energy resolution of $10^{-4} < \Delta E/E < 10^{-2}$ due to the long flight path, low background and the large time interval between the proton bunches, minimizing the possibility of overlapping neutrons from successive bunches.

The detector used was a Fast Ionisation Chamber (FIC) with fast timing properties, especially built at CERN for measuring neutron induced fission on minor actinides at the n_TOF facility [5]. It consists of a stack of cells mounted one after the other with respect to the beam direction, filled with Ar (90%) + CF₄ (10%) at a pressure of 720 mbar. Each cell consists of three electrodes. The central Al electrode, of 100 μm thickness, was actually the backing of the actinide targets and in most of the cases it was plated on both sides with a disk of actinide target. The external electrodes, of 15 μm thickness, are used to define the electric field at 600 V/cm in the active gas-filled volume of the detector. In this way two separate active detection volumes are created but the corresponding signals are taken through the same DAQ channel, so at the end there is one signal coming out from each cell. The stack of cells was put in a sealed Al chamber. The total attenuation of the neutron fluence through the stack of cells was estimated with Monte Carlo simulations to be less than 1%, while the background induced by scattered neutrons in the materials of the detector was found to be negligible [5].

An innovative data acquisition (DAQ) system based on fast digitizers has been developed [10]. The main feature of this system is the possibility to sample and record the full analogue waveform of the detector signal in digitized form, for off-line analysis. The sampling was performed by means of fast Flash Analogue to Digital Converters (FADC) and the detector signals were recorded in 4096 bins of 25 ns width in a time window of 100 μs (“movie”) which corresponds to neutron energies from GeV down to ~ 20 keV. A typical movie obtained from the runs can be found in fig. 1.

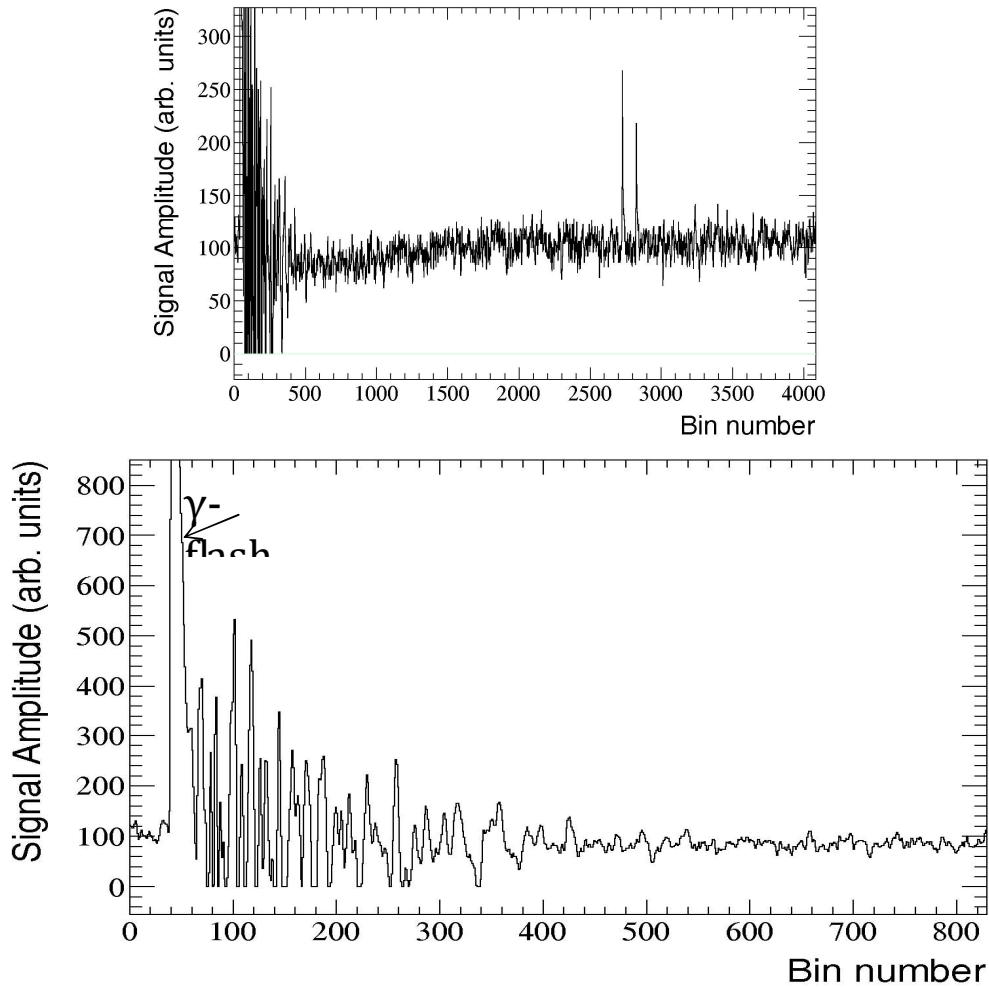


Fig. 1. A typical movie obtained from one neutron bunch, recorded in 4096 bins of 25 ns width in a time window of 100 μ s. Upper figure: The whole movie where 2 fission fragment (FF) pulses were recorded at bins 2725 ($E_n \sim 39$ keV) and 2825 ($E_n \sim 37$ keV). Lower figure: The same movie zoomed in the early phase, where the γ -flash signal and the oscillations and saturations of the baseline can be seen.

The first large signal (at bin 62 in fig. 1) occurs from large energy deposition of gamma rays and relativistic particles produced from the spallation processes and arrive first at the experimental area (“ γ -flash”). This signal is used for the accurate estimation of the time-of-flight of the neutrons. However, it causes malfunctions in the electronic chain of the detector, so the baseline of the signal after the γ -flash peak presents intense rippling and undershooting. The distortion is so large that causes signal saturation at some bins, where data cannot be recovered, especially for neutron energies bigger than 9 MeV, which is the upper neutron energy limit for which safe cross section data results could be extracted.

3. Analysis procedure

An efficient method for analysing the data in an automated way was used [6,11] in order to provide a reliable background subtraction and identification of FF events even at high energies, based on pulse shape analysis techniques. The background subtraction is based on the observation that all the movies follow the same baseline pattern in this region, so an average FADC output (“average movie”) was produced and after a linear fitting on

each event under analysis it was subtracted from the latter. Thus, in the resulting event the unwanted oscillations and the baseline undershooting were removed. Then, the fitting of the FF peaks was easily and more accurately performed even if they were initially lying on an oscillating background. An example of the analysis is shown in fig. 2.

A separate analysis was performed for each target in order to estimate the accepted limits of the fitting parameters and their errors, by checking the raw data. More than 300000 events were accepted for each target and amplitude histograms of the accepted FF pulses were obtained, as the one shown in fig. 3.

The sensitivity of the analysis results on the change of various parameters was tested (e.g. threshold, background level, grouping of movies for the extraction of the average movie) and it was found out that the changes within meaningful limits had a small influence mainly at the low amplitude pulses. For this reason an analysis threshold was applied in order to cut these low energy pulses.

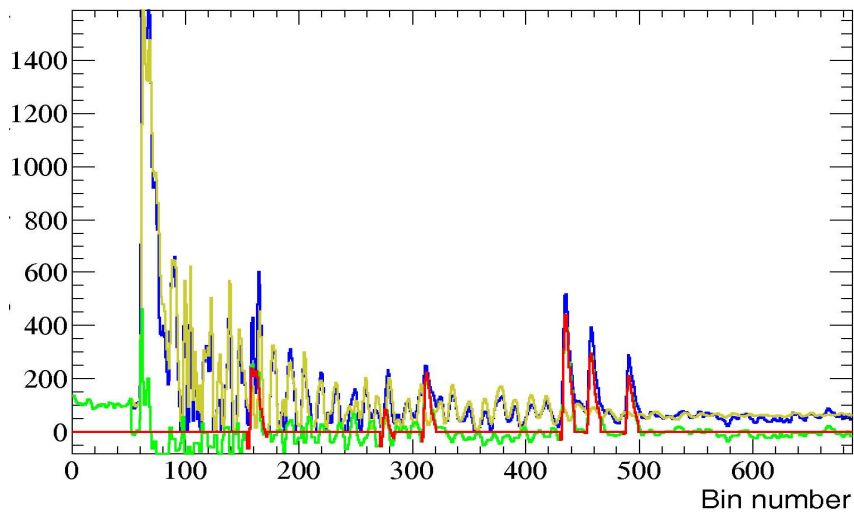


Fig. 2: Example of the analysis of one FADC movie. The blue line corresponds to the raw data, the yellow line to the fitted average movie and the green line to the remaining movie after the subtraction of the fitted average movie. The red line corresponds to the FF peaks that were recognised and fitted by the code.

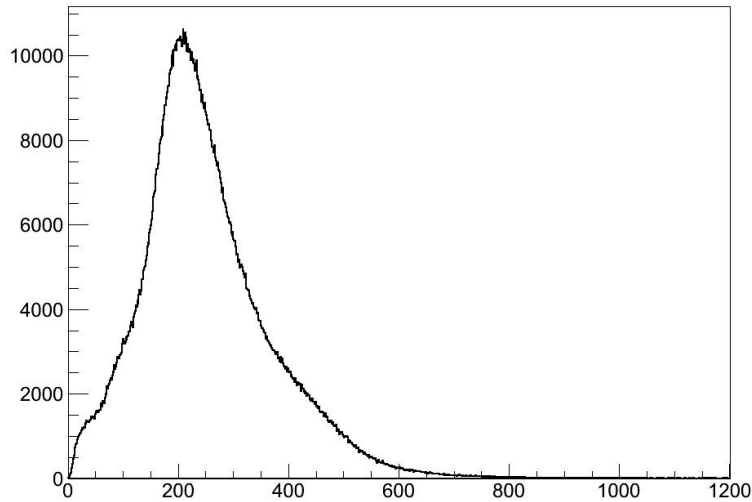


Fig. 3: Amplitude distribution of the accepted FF peaks for the ^{237}Np target. The resolution obtained due to the fast electronics used does not allow the separation between the heavy and light FF peaks.

The cross section was calculated with use of the formula 1, with reference to the $^{235}\text{U}(n,f)$ reaction cross section for neutron energies < 2 MeV and the $^{238}\text{U}(n,f)$ reaction cross section above that value:

$$\sigma_{\text{Np7}(n,f)} = \frac{C_{\text{Np7}} N_t \text{ref} n\text{Events}_{\text{ref}} \text{eff}_{\text{ref}}}{C_{\text{ref}} N_t \text{Np7} n\text{Events}_{\text{Np7}} \text{eff}_{\text{Np7}}} \sigma_{\text{ref}} \quad (1)$$

C is the number of counts for the corresponding target, corrected for the FF counts below the analysis threshold with use of Monte Carlo simulations with the code FLUKA [12] and eff the detection efficiency also estimated with the FLUKA simulations. An external routine provided the generation of the FFs with mass and atomic numbers and energies based on systematics [13,14], which were homogeneously distributed in the target volume and their energy deposition in the active volume of the gas was scored. A typical simulated energy deposition histogram without the response function of the detector is shown in fig. 4. The efficiency corrections and the correction for subthreshold FF counts did not exceed 3.5% and 5.6% respectively in the worst case (for the thicker target).

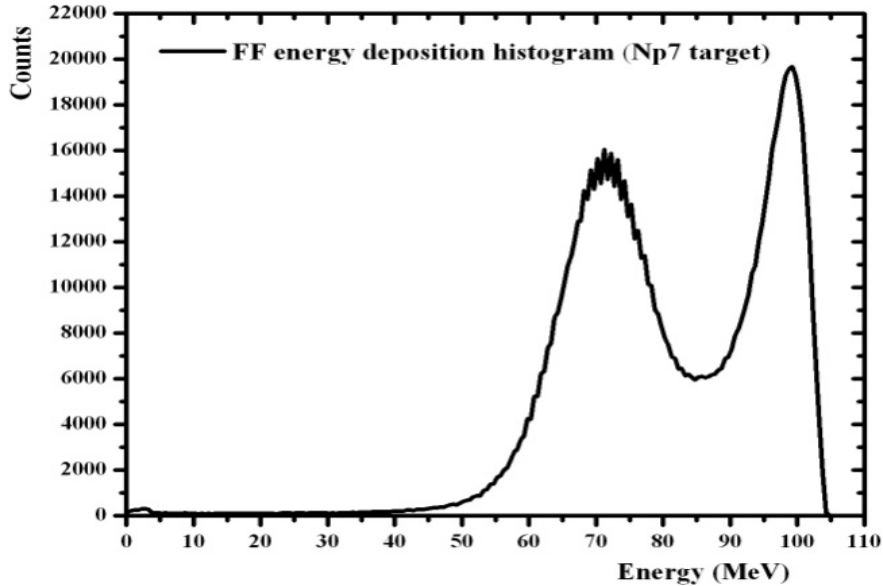


Fig 4: The energy deposition histogram of the FFs in the active detector volume obtained from the FLUKA simulations, for the thinnest target (^{237}Np target).

The surface density of the targets (N_t in equation 1) was determined with alpha spectroscopy with use of SSB detectors as explained in [15]. The surface density of the actinide of interest in the targets was < 0.5 mg/cm^2 , while the corresponding surface density of the impurities was $< 10^{-6}$ mg/cm^2 , thus the targets can be characterised as of high purity. Furthermore, the thickness and homogeneity of the targets was examined with the Rutherford Backscattering Spectrometry Technique using an external proton beam at the I.N.P.P of the NCSR “Demokritos” and the targets were found to be homogeneous at satisfactory levels [15].

In order to check and validate the various components of the analysis the $^{238}\text{U}(n,f)$ was calculated, with reference to the $^{235}\text{U}(n,f)$ reaction and a good reproduction of ENDF/B-VII.1 was achieved.

4. Cross section results

The $^{237}\text{Np}(n,f)$ cross section results obtained with the above mentioned analysis are compared to the latest data in a wide energy range [16] and the latest evaluations ENDF/B-VII.1 [1] and JEFF 3.2 [2] in fig 5. As a general remark, the data obtained from this work are in agreement with the latest data and the evaluations at the first chance fission threshold but above that value they are slightly systematically lower than the latest data of [16] although they were measured at the same facility. The data from the present work generally seem to agree with the latest evaluations in the whole energy range.

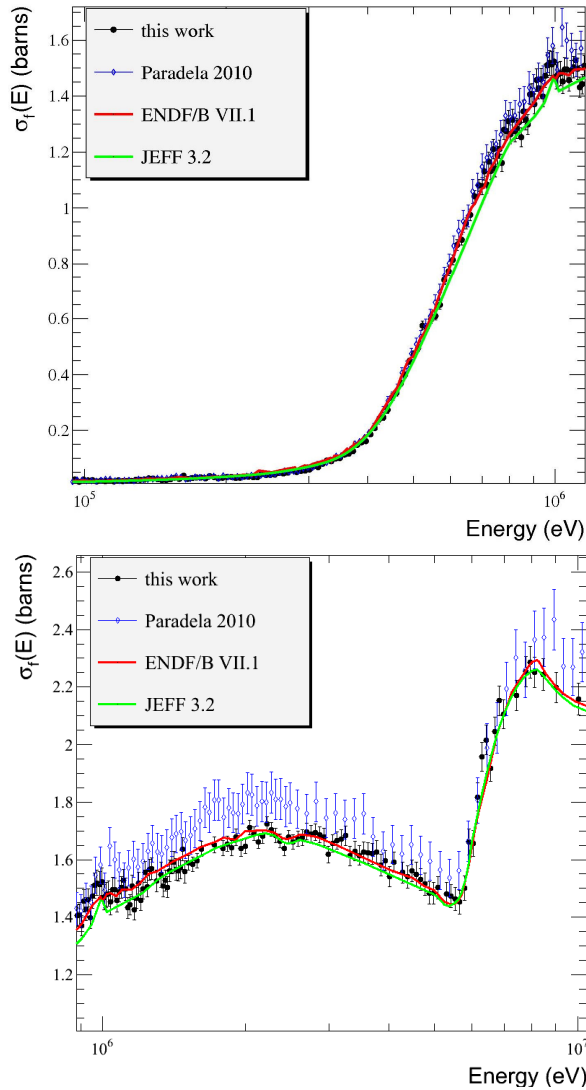


Fig 5: The cross section results from this work compared to the latest data and evaluations. Upper figure: The energy range 10 keV -1 MeV is shown, which corresponds to the first chance fission threshold. Lower figure: The energy range 1 MeV -10 MeV is shown, which corresponds to the plateau of the first chance fission and the second chance fission threshold.

5. Theoretical calculations with the EMPIRE code

The reproduction of the $^{237}\text{Np}(n,f)$ cross section results in the energy range 100 keV - 10 MeV was attempted with phenomenological models using the code EMPIRE, version 3.2

– Malta \ref{empire,empire3.2}. The calculations were performed within the Hauser-Feshbach formalism, with fission being an open exit channel competing only with neutron induced reactions (such as (n,γ) , (n,el) , (n,inl) , $(n,2n)$ in the neutron energy range of interest). The transmission coefficients for the entrance and neutron exit channels were calculated with the Optical Model RIPL-2408 (Koning-Delaroche), while for the fission exit channel the transmission is calculated through a double humped barrier. The level density model both for the normal and the transition states was the Enhanced Generalised Superfluid Model which has been proven to work fine for nuclei in the actinide region. Concerning the fission channel, drastic changes at the heights and widths of the fission barriers, as well as the level density parameters of the transition states continuum, mainly for the nuclei ^{238}Np and ^{237}Np , were needed in order to better reproduce the data. Preliminary results are shown in fig. 6, where the theoretical calculations of the fission channels and the competing reaction channels are shown, in comparison with existing data found in the EXFOR database [17] and in the case of the (n, el) with the ENDF/B-VII.1 evaluation [1], since no data were found in EXFOR.

The calculated cross section values reproduce quite well the experimental data of the fission reaction and of the main competing channels in the biggest part of the energy range of interest. Nevertheless, in the energy range 1- 2 MeV there is an overestimation of the fission cross section by 20%. Various tests were made to further decrease the calculated fission cross section in this region without clearly improving this energy region and at the same time keeping the good reproduction at the other energy regions. A possible solution would be to adjust the discrete transition states on the first and second saddles of the ^{238}Np barriers since they severely affect this energy region, but this needs special care and will be further investigated.

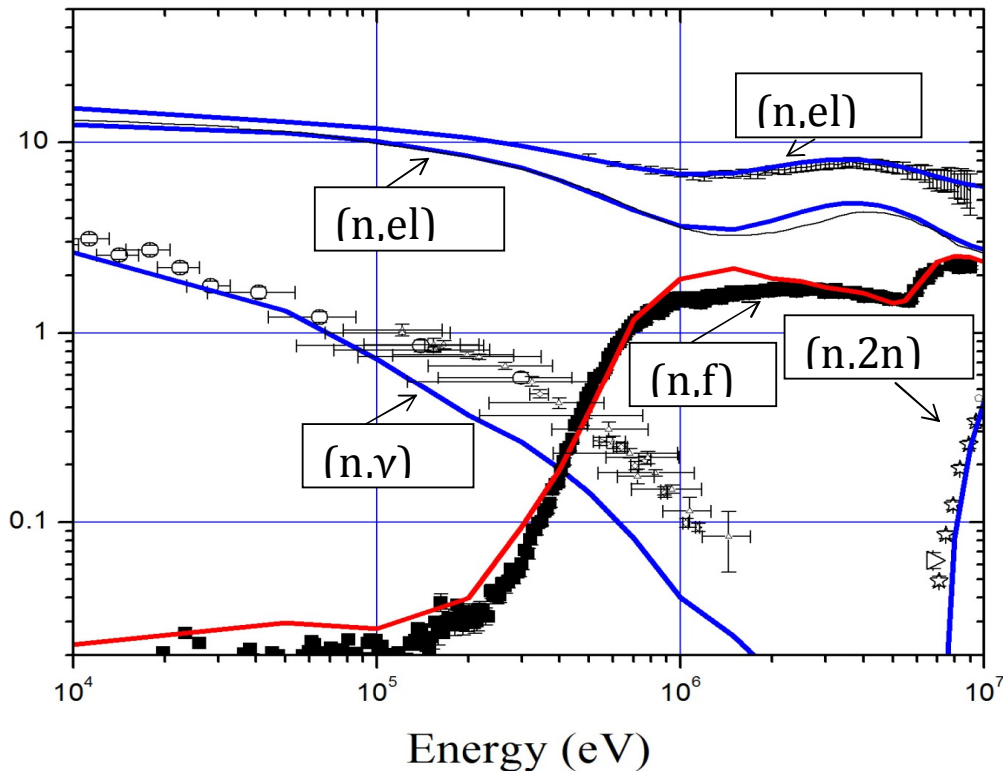


Fig 6: The preliminary calculated cross section results with EMPIRE for the fission channel (red line) as well as the main competing reaction in the energy range 10 keV- 10 MeV (blue lines): (n,γ) , (n,el) , (n,inl) , $(n,2n)$. The data points correspond to the n_TOF cross section data obtained from this work for the fission channel and to the experimental data found in EXFOR for the competing reactions. The black line corresponds to the ENDF/B VII.1 evaluation for the (n,el) channel.

6. Summary

The cross section of the $^{237}\text{Np}(n,f)$ was measured at the n_TOF facility at CERN in the energy range 10 keV - 9 MeV with a Fast Ionisation Chamber, and the results are approximately 7% lower than the latest data measured at the same facility. The reproduction of the experimental data obtained from this work was attempted within the Hauser-Feshbach formalism with use of the code EMPIRE 3.2, limiting the results by the simultaneous reproduction of the main competing reaction channels in the energy range of interest. The theoretical investigation gave results that generally agree with the experimental data but it is ongoing and needs to be finalised.

Acknowledgements

This research has been co-financed by the European Union (European Social Fund - ESF) and Greek national funds through the Operational Program "Education and Lifelong Learning" of the National Strategic Reference Framework (NSRF) - Research Funding Program: Heracleitus II. Investing in knowledge society through the European Social Fund.

References

- [1] M. B. Chadwick et al, Nuclear Data Sheets 112 (2011) 2887-2996.
- [2] JEFF-3.2, Evaluated Data Library (neutron data), OECD Nuclear Energy Agency, 2014.
- [3] K. Shibata, et al., "JENDL-4.0: A New Library for Nuclear Science and Engineering," J. Nucl. Sci. Technol. 48(1), 1-30 (2011).
- [4] "CERN n_TOF Facility: Performance Report", CERN/INTC-O-011,INTC-2002-037,CERN-SL-2002-053 ECT, 2002.
- [5] M. Calviani et al, Nucl. Instr. Meth. A 594 (2008) 220.
- [6] D. Karadimos et al. (the n_TOF collaboration), Nucl. Instr. Methods in Phys. Res. B 268 (2010) 2556-2562.
- [7] "EMPIRE: Nuclear reaction model code system for data evaluation", M. Herman, R. Capote, B. V. Carlson, B. Oblozinsky, M. Sin, A. Trkov, H. Wienke and V. Zerkin, Nucl. Data Sheets 108 (2007) 2655-2715.
- [8] EMPIRE-3.2 Malta, M. Herman, et al., INDC(NDS)-0603, BNL-101378-2013.
- [9] C. Rubbia, et al., A high resolution spallation driven facility at the CERN-PS to measure neutron cross-sections in the Interval from 1 eV to 250 MeV, CERN/LHC/98-02 (EET).
- [10] U. Abbondanno et al., the ntof collaboration, Nucl. Instr. Methods in Phys. Res. A 538 (2005) 692-702.
- [11] D. Karadimos et al., Phys. Rev. C 89, 044606 (2014).
- [12] "FLUKA: a multi-particle transport code", A. Ferrari et al., CERN-2005-10 (2005), INFN/TC_05/11, SLAC-R-773.
- [13] G. D. Adeev et al, Preprint INR RAS 861/93, 1993.
- [14] F.-J. Hamsch et al, Nucl. Phys. 679 (2000) 3-24.
- [15] M. Diakaki et al., Proceedings of the 21st Symposium of the Hellenic Nuclear Physics Society (2012) 81-88.
- [16] C. Paradela, et al, the n_TOF collaboration, Phys. Rev C 82, 034601 (2010).
- [17] <http://www.nndc.bnl.gov/exfor>.